Journal of Metals, Materials and Minerals, Vol.29 No.1 pp.22-30, 2019

Effect of carbon addition on microstructure and properties of boron-containing steel sintered under different atmospheres

Wantana KOETNIYOM[1,2], Pisamorn CHANTAWET[1], Nattaya TOSANGTHUM[3,*], Monnapas MORAKOTJINDA[3], Thanyaporn YOTKAEW[3], Pongsak WILA[3], and Ruangdaj TONGSRI[3]

[1]*Department of Industrial Physics and Medical Instrumentation (IMI), Faculty of Applied Science, King Mongkut University of Technology North Bangkok, Bangkok 10800, Thailand*
[2]*Lasers and Optics Research Center (Landos), King Mongkut University of Technology North Bangkok, Bangkok 10800, Thailand*
[3]*Particulate Materials Processing Technology Laboratory (PMPT), Thailand National Metal and Materials Technology Center, 114 Paholyothin Road, Khlong Nueng, Khlong Luang, Pathum Thani 12120, Thailand*

***Corresponding author e-mail:** nattayt@mtec.or.th

Received date:
19 May 2018
Revised date:
4 February 2019
Accepted date:
8 February 2019

Keywords:
Liquid-phase sintering
Sintering atmosphere
Deboronization
Sintered steels

Abstract

High performance sintered steels can be obtained by simultaneous tailoring microstructural feature and improving sintered density. Although sintered hardening is used to produce sintered components with microstructural features providing high tensile strength and hardness, but the performance is limited by low ductility due to the presence of porosity. Near full density can be achieved by liquid phase forming as a result of boron addition to a sintered steel. A liquid formed due to the eutectic reaction of Fe + Fe_2B, spreads to interparticle spaces leading to densification improvement. Carbon is an indispensable element for high strength sintered steels. It plays important roles in both matrix microstructural development and intergranular liquid phase formation. This work has investigated the sintered Fe-1.5Mo-0.22B-*x*C steels (*x* = 0.1 - 0.4 wt.%) sintered under hydrogen and vacuum atmospheres. It was found that the hydrogen-sintered Fe-1.5Mo-0.22B-*x*C steels hardly showed evidences of intergranular liquid phase whereas all experimental vacuum-sintered steels showed intergranular boride. Deboronization is believed to contribute to the intergranular boride absence in the hydrogen-sintered steels. However, when the hardening effect was taken into account, the strengthening by intergranular liquid phase in the sintered steels was less important than precipitation strengthening. Advantage of ductility was only obtained in the vacuum-sintered steels with C contents ≤ 0.1 wt.%, whose microstructures contained discontinuous boride networks along polygonal ferrite grain boundaries. In contrast, the presence of continuous and thick boride networks caused embrittlement to the sintered steels.

1. Introduction

Near net shape powder metallurgy (PM) steels (low carbon (C) iron (Fe)-based alloys) have significant growth in the automotive industry. They are extensively used as gears, sintered magnets, self-lubricating bearings and other complex structural components due to their benefits such as cost effectiveness, weight and energy savings and uniformity in shapes and dimensions. Although sintered hardening is used to tailor the microstructure of sintered products that acquire the desired mechanical performance by optimizing the material composition and cooling rate but their applications are limited with loss in ductility due mainly to the presence of porosity which generally ranges from 5 to 10 vol. %. In order to expand the scope of sintered part applications, improvement in sintered density without considerably increasing the production cost by liquid-phase sintering (LPS) is a versatile method. Amongst several additive additions, boron (B) is now widely accepted for obtaining high density in PM steels. Liao et al. [1] reported that B significantly improved the density of the PM steels by forming a liquid with iron at ~1447 K (1174 °C) due to the

DOI: 10.14456/jmmm.2019.4

eutectic reaction γ-Fe + Fe_2B → L. The liquid form spreads into interparticle spaces, particle rearrangement due to capillary forces contributes to densification results in a final microstructure consisting of a B-rich phase network surrounding the grains boundary. However, sintered plain carbon steel rarely uses LPS because the Fe-B eutectic at the grain boundaries is a fairly brittle phase. Once high density is achieved, the material is brittle [2]. According to experimental results, Sercombe et al. [3] concluded that B-containing PM steels are suitable materials for LPS densification to achieve wear resistant materials with a low porosity.

Hardenability alloying elements such as Cr, Mo and C have important roles in the progress of LPS and the final densification in B-containing PM steels. B can form stable phases with some elements resulting in alteration of the phase composition in both matrix and boride network which affect the mechanical property. Various compound phases, including M_2B, M_3B_2, M_7C_3, $M_3(B,C)$, and $M_{23}(B,C)_6$, wherein M comprises one or more of the metallic elements, including Fe, Cr, Mo, could be present in the B-containing PM steels, depending on the steel compositions and process parameters [3,4,5]. Many researches have shown the effects of various alloying elements on the LPS behavior, sintered density, and microstructures. Wu [6] reported that, although the increase of B content in PM alloyed steels could promote LPS densification and porosity reduction but in some cases, the tensile strength and elongation were decreased due to inadequate microstructures. Wu et al. [7] found that Mo and Cr atoms could stabilize M_2B boride, where M represents the metallic elements Fe, Mo, and Cr, at a higher temperature. In addition, they found that adding 0.5 wt% C to Fe-0.4B and Fe-1.5Cr-0.4B steels could reduce the temperature of liquid formation by ~5 °C and ~50 °C, respectively, and could enhance the LPS densification. Liu et al. [8] showed that the sintered density of Fe-1Ni-1Mo-xC-0.3B steel was not obviously changed by a C content of up to 0.4 wt.% C. In contrast, Xiu et al. [9] indicated that the sintered density of Fe-Mo-C-B steel is improved by increasing the C content from 0.2 wt% to 0.44 wt.%.

Recently, sintered Fe-Cr-Mo-BN-C steels, produced by admixing of hexagonal boron nitride (h-BN) and graphite to pre-alloyed Fe-3.0Cr-0.5Mo powder, sintering in vacuum atmosphere, and cooling with different rates, showed benefits of higher strengths [10]. A few researches have been conducted for atmospheric effects on B-induced LPS of steel powder compacts. It was reported that a considerable amount of B removal was observed during the heat treatment of Fe-36%Ni and Fe-78%Ni alloys at 1050°C in different atmospheres [11]. Because of deboronization possibility in some atmospheres and the roles of carbon in the LPS of B-containing PM steel have not yet been fully identified. In order to ensure the successful liquid phase sintering by B addition, this work has devoted to investigate the Fe-1.5Mo-0.22B-*x*C steels (x = 0.1 - 0.4 wt.%) sintered under hydrogen and vacuum atmosphere.

2. Experimental

Water-atomized steel powder pre-alloyed with 1.5 wt.% Mo is commercially available as Astaloy Mo from Höganäs AB, Sweden. It was admixed with fixed 0.5wt.% h-BN and varied contents of 0.0-0.4 wt. % C with 0.1% step wise increment. Addition of 1 wt.% zinc stearate was also conducted in order to lubricate the compact and the pressing die. After admixing, green "dog-bone" compacts were produced by pressing at 450 MPa to obtain green density of 6.5 g/cm^3, following the ASTM standard B 925-03 (Standard Practices for Production and Preparation of Powder Metallurgy (P/M) Test Specimens). The density was measured by the water displacement method as given in Standard 42 (Determination of density of compacted or Sintered Powder Metallurgy (PM) Products). Sintering was carried out under atmospheres of pure hydrogen (the flow rate of 200 L·h^{-1}) and vacuum (10^{-9} mbar) atmosphere at 1280°C for 45 min and then cooled in the furnace with the rate of 0.1°C·min^{-1}. For metallographic examination the specimens, exposing a cross-sectional view, were polished and etched with a solution of 2% Nital. Microstructural features were observed by means of light optical microscopy (OM) and scanning electron microscopy (SEM) under Hitachi SU 8230 microscope. Energy dispersive x-ray spectroscopy (EDS) was used for elemental analysis. Tensile properties were tested by following the MPIF Standard 10 (Determination of the Tensile Properties of Powder Metallurgy (PM) Materials). The test was conducted by using Instron Universal testing machine using a strain rate of 5 mm·min^{-1}. Micro-hardness studies were performed using Vicker's micro-hardness tester.

3. Results and discussion

3.1 Microstructures

Microstructures of the sintered steels with compositions of Fe-1.5Mo-0.22B-*x*C (*x* = 0.1-0.4 wt.%), produced from Fe-1.5Mo + 0.5h-BN + *x*C powder mixtures and sintered under vacuum atmosphere, are shown in Figure 1. They were observed by using OM as shown in Figure 1(a, b, c) and SEM as shown in Figure 1(d, e, f). It was found that microstructures of the vacuum-sintered steels without carbon addition consisted of polygonal ferrite (PF) grains (Figure 1(a, d)), pores and intergranular boride. The latter phase was observed

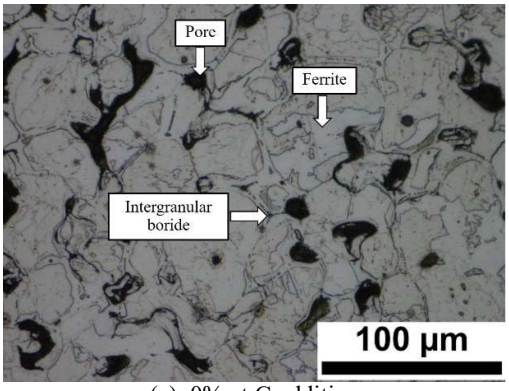

(a) 0%wt.C addition

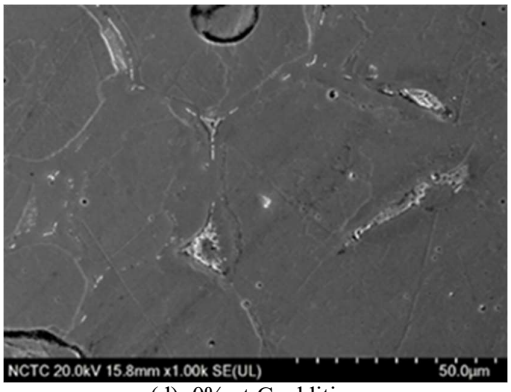

(d) 0%wt.C addition

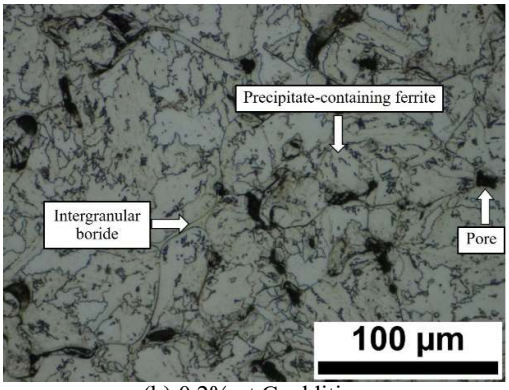

(b) 0.2%wt.C addition

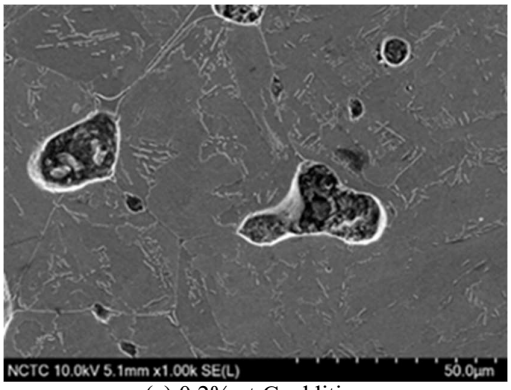

(e) 0.2%wt.C addition

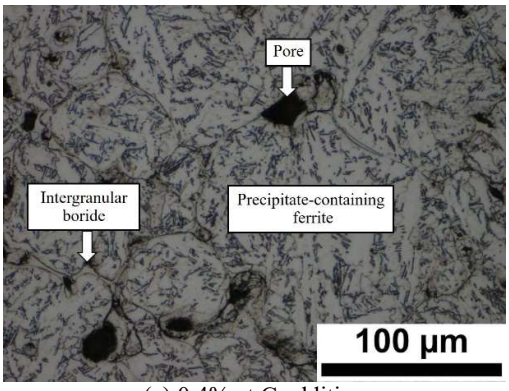

(c) 0.4%wt.C addition

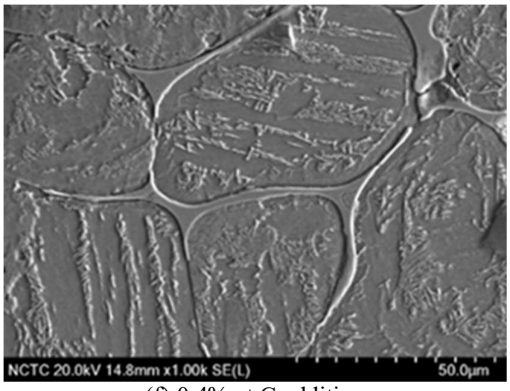

(f) 0.4%wt.C addition

Figure 1. Images of Fe-1.5wt.% Mo + 0.5wt.% h-BN sintered at 1280ºC for 45 min. under vacuum atmosphere with variation of C addition observed by OM (a,b,c) and SEM (d,e,f).

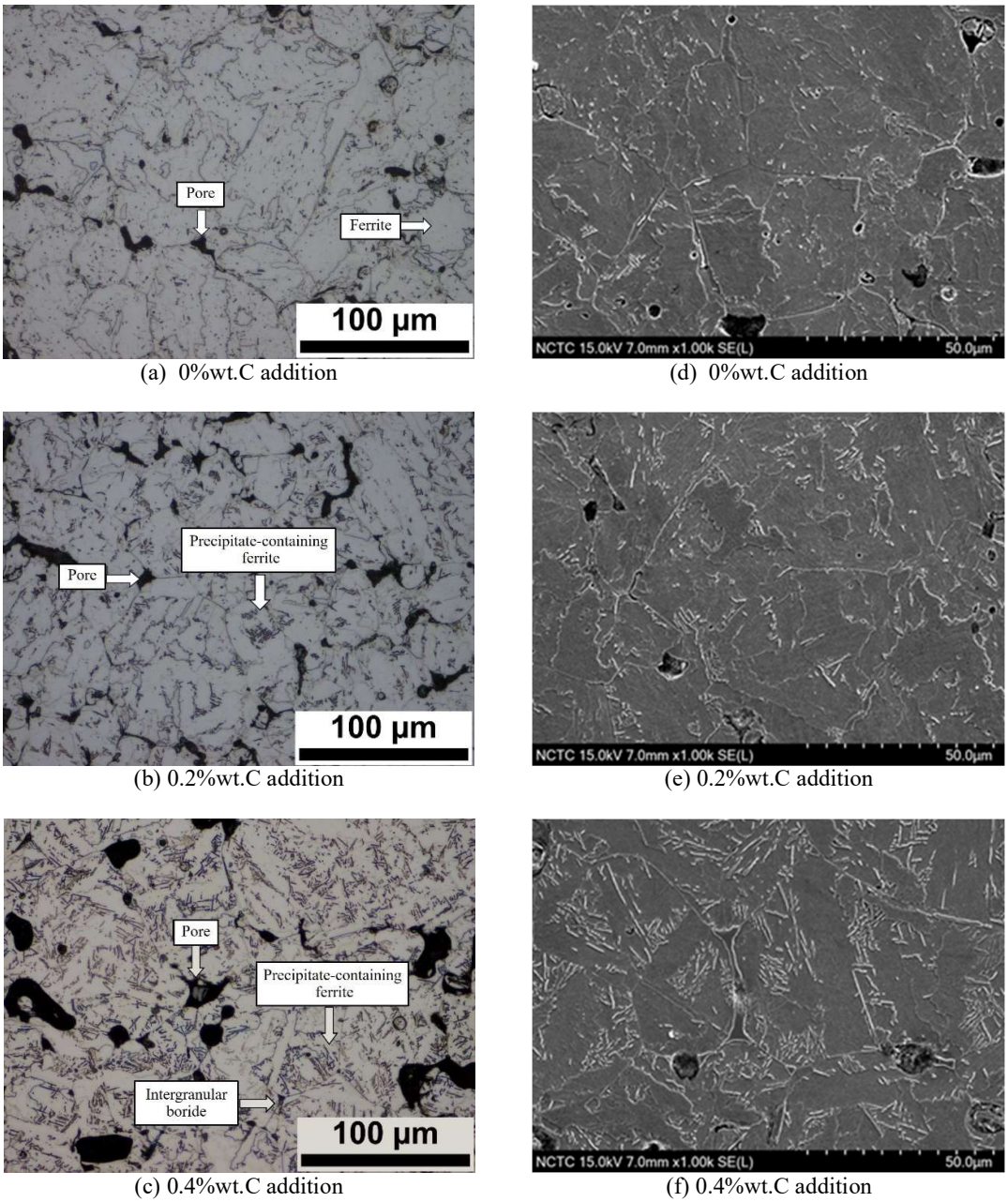

(a) 0%wt.C addition (d) 0%wt.C addition

(b) 0.2%wt.C addition (e) 0.2%wt.C addition

(c) 0.4%wt.C addition (f) 0.4%wt.C addition

Figure 2. Images of Fe-1.5wt.% Mo + 0.5wt.% h-BN sintered at 1280ºC for 45 min. under hydrogen atmosphere with variation of C addition observed by OM (a,b,c) and SEM (d,e,f).

at the triple junction and near some pores. The volume fraction of intergranular phase resulting from liquid solidification increased with increasing C content. The material grain morphology changed from clean PF grains (Figure 1(d)) to precipitate-containing grains (Figure 1(e, f)) when C contents were increased. Precipitation along lath ferrite boundaries was observed in the sintered Fe-1.5Mo-0.22B-0.4C steel (Figure 1(f)). Liquid phase sintering occurs in the vacuum-sintered steels as evidenced by (i) the presence of intergranular boride, (ii) round grains and round pores (Figure 1).

The solubility of B in Fe is limited, thus sintering at a temperature higher than 1200°C (1473 K) conduces to the formation of a liquid boride phase [12]. The liquid phase is generated as a result of eutectic reaction between Fe and Fe_2B. The reactions are $Fe + Fe_2B \rightarrow L$ for Fe-B system and $(Fe, Mo) + (Fe, Mo)_2B \rightarrow L$ for Fe-Mo-B system [13]. The volume fraction of intergranular boride

also increased with increasing carbon addition same as the result of Sundaram et al. [13] indicated that both carbon and molybdenum accelerate sintering by promoting the formation of liquid at a much lower temperature. The C addition as admixed graphite can shift liquid formation temperature to a lower one that also contributes to the higher liquid volume fraction resulting in better densification.

Microstructure of the hydrogen-sintered steels are shown in Figure 2. It was found that intergranular liquid phase was hardly observed. The fraction of precipitation in the hydrogen-sintered steel matrix was increased with increasing C content (Figure 2 (d, e, f)). The precipitates in the hydrogen-sintered steels dispersed rather randomly compared to that in the vacuum-sintered steels (Figure 1(f) and 2(f)).

The absence of the intergranular liquid phase is consistent with the previous study on deboronization possibility in some atmospheres. According to Tsuda [11], a considerable amount of B removal was observed during the heat treatment of Fe-36%Ni and Fe-78%Ni alloys at 1050°C in air. Neither argon nor hydrogen (dew point -40°C) atmosphere could eliminate the deboronization. Hence, deboronization is believed to contribute to the intergranular boride absence in the hydrogen-sintered steels.

With comparison between the microstructures of vacuum- and hydrogen-sintered steels, the intergranular liquid phase was absent in the latter whereas the amount of precipitates, increases with increasing carbon addition in both sintered steels. It is implied that sintering atmosphere types strongly influence on intergranular liquid phase formation but insignificantly influence on precipitation in sintered steel matrix.

As far as the sintered density is concerned, sintered densities were improved to values higher than 7.0 $g \cdot cm^{-3}$ from the green density of 6.5 $g \cdot cm^{-3}$. The plot of sintered density against added graphite (C) content, given in Figure 3, indicates that the hydrogen-sintered steels show increase of sintered density with C contents of up to 0.3 wt. %, whereas the vacuum-sintered steels show non-systematic relationship with C content. The added C content has two roles in densification of a sintered steel specimen. As given above, C promotes formation of liquid phase, which enhances densification by liquid phase sintering [13]. This role of carbon should be applied with caution. For example, in case of insufficient liquid phase quantity, the penetration of a liquid phase to wet a small gap between powder particles by capillary effect will leave porosity behind. This means that a small amount of liquid can reduce densification of a sintered specimen. That is why the vacuum-sintered steels show non-systematic relationship with C content. The second role of C on sintered part densification is that C acts as oxide-reducing agent during heating a metal powder compact [14]. Metal powder surface oxides, entrapped inside the inter-particle contact areas as the potential areas for sintered neck formation, can be removed by presence of graphite. The C addition, in combination with hydrogen as effective reducing agent, is expected to produce better densitication.

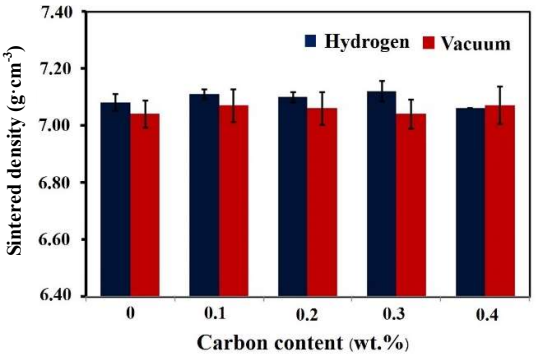

Figure 3. Sintered density of experimental sintered steels.

Figure 4 shows the distribution of major elements in the steel matrix and intergranular boride. As seen, the boride was enriched with Fe and Mo, while the precipitates in the matrix were enriched with C. However, the EDS analysis is not suitable for detecting low content of light elements like B.

According to literatures [3-5], various compounds, including M_2B, M_3B_2, M_7C_3, $M_3(B,C)$, and $M_{23}(B,C)_6$, wherein M comprises one or more of the metallic elements, including Fe, Cr, Mo, could be present in sintered B-containing steels, depending on the steel compositions and process parameters. Due to C enrichment at precipitate sites in the matrix, they are presumably cementite (Fe_3C) and other carbides (M_7C_3, $M_3(B,C)$, and $M_{23}(B,C)_6$).

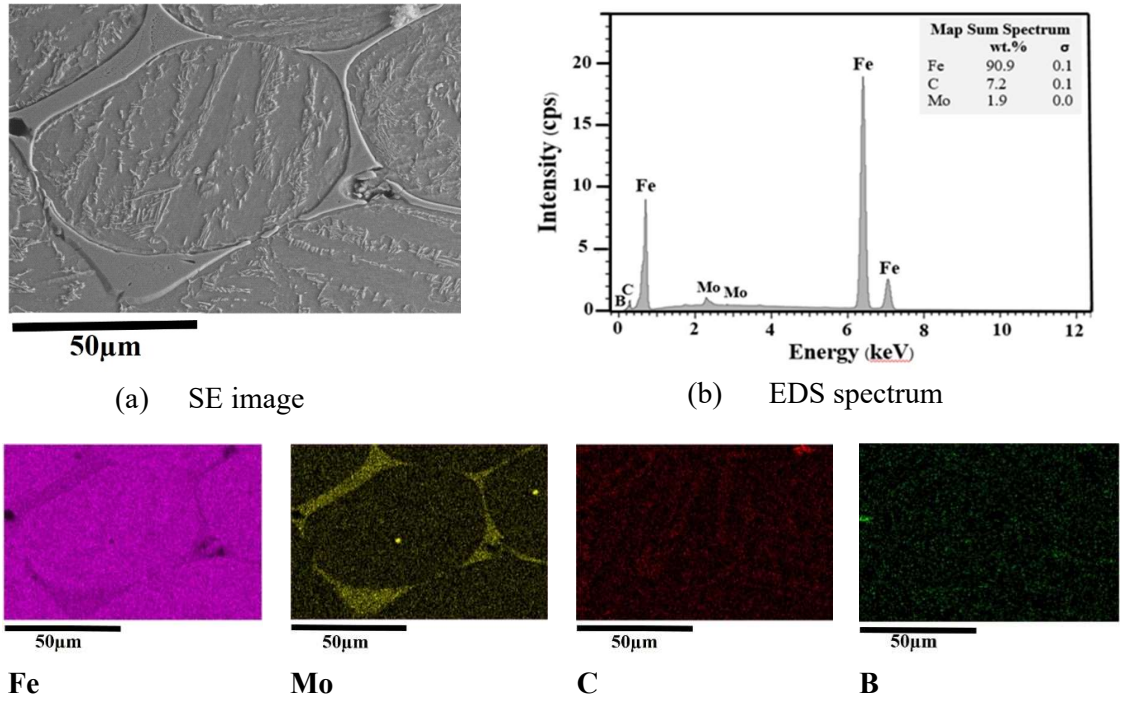

Figure 4. X-ray mapping of element distribution in Fe-1.5wt.% Mo + 0.5wt.% h-BN + 0.4wt.% C sintered at 1280ºC for 45 min. under vacuum atmosphere.

3.2 Mechanical Properties

Figure 5 showed mechanical properties of the vacuum and hydrogen sintered specimens. Tensile strength (Figure 5(a, b)) and hardness (Figure 5(d)) of both sintered steel types increased with increasing C content. There was insignificant difference in tensile strength and hardness compared between both sintered steel types. The common feature of both sintered steel types is precipitation inside the matrix. Volume fraction of precipitates also increased with increasing C content. Thus, the strengthening phenomena in both sintered steel types is attributed to precipitation hardening.

The other reason for tensile strength increase in the vacuum-sintered specimens with high C contents (> 0.1 wt.%) is ferrite morphology. The difference in ferrite morphology can be compared between the vacuum-sintered specimen (Figure 1(f)) and the hydrogen-sintered specimen (Figure 2(f)). In the former specimen, ferrite has lath shape with precipitates decorating its boundary. In contrast, the ferrite in latter specimen preserves its polygonal shape with precipitates dispersing randomly inside it. The change of ferrite grain morphology from coarse polygonal to lath shape provides the hardening effect to a steel [15].

Marked difference was observed for the sintered steel ductility (Figure 5(c)). The ductility of the sintered steels was dependent on both sintering atmosphere and C content. With C contents ≤ 0.1 wt.%, the vacuum-sintered specimens showed elongation higher than that of the hydrogen-sintered specimens. Since both sintered low C steels have insignificant amount of precipitates inside the matrix, the ductility difference is owing to the presence of the intergranular liquid phase, which shows a discontinuous network along grain boundaries (Figure 1(d)). This result conforms to the study of Vassileva et al. [16] published that the formation of a discontinuous eutectic network along the grain boundaries can improve ductility. With C contents > 0.1 wt.%, the vacuum-sintered specimens showed elongation lower than that of the hydrogen-sintered specimens. The continuous and coarse intergranular liquid phase in the vacuum-sintered specimens (Figure 1(f)) is the cause of ductility reduction. Sandaram et al. [13] reported that although C and Mo additions can promote the volume fraction of liquid that contributes significantly to densification but not necessarily

the mechanical properties as it results in embrittlement. Kazior et al. [17] reported that carbon has significant effect on the tensile properties of sintered Fe-Cr-Mo-B steels. Yield strength increased from 463 MPa to 509 MPa, Ultimate tensile strength (UTS) increased from 613 MPa to 666 MPa and elongation decreased from 1.99 % to 1.74 % with C addition. The higher values compare to the result of this work due to different chemical composition of specimens, pressing and sintering condition. The trend is that, the higher carbon content, the higher are the yield, strength, hardness and lower elongation.

High volume fraction of precipitates, presumably cementite and other carbides, indicates that there is low soluble C content in the sintered steel matrix. Since chemical stabilization due to the enrichment of carbon in the retained austenite is the most important operational mechanism for the austenite retention [18,19], the low soluble C content in the sintered steel matrix available for retained austenite stabilization indicates an inadequate amount of retained austenite. High strength steels with microstructures containing lath ferrite or martensite will have a considerable ductility if a suitable volume fraction of retained austenite is present and the transformation induced plasticity (TRIP) effect [20-22] performs during deformation process. The shortage or insufficient volume fraction of retained austenite will cause the material be brittle.

4. Conclusions

In this study, C additions were varied to observe their effects on the liquid formation, steel matrix and mechanical properties of the sintered Fe-1.5Mo-0.22B-*x*C steels (x = 0.1-0.4 wt. %) sintered under hydrogen and vacuum atmospheres. The microstructural features are clearly dependent on the amount of carbon addition. Carbon plays important roles in both matrix microstructural development and also intergranular liquid phase formation. Increasing C addition tends to increase tensile properties and micro hardness. The decrease of elongation is due to dispersed precipitates in the matrix and formation of thick continuous network of boride structures along the grain boundaries. The results demonstrated that no significant difference in mechanical properties between vacuum and hydrogen atmosphere. Deboronization is believed to contribute to the intergranular boride absence in the hydrogen-sintered steels. Although the presence of intergranular liquid phase, the number of pores were still observed, possibly due to insufficient B content.

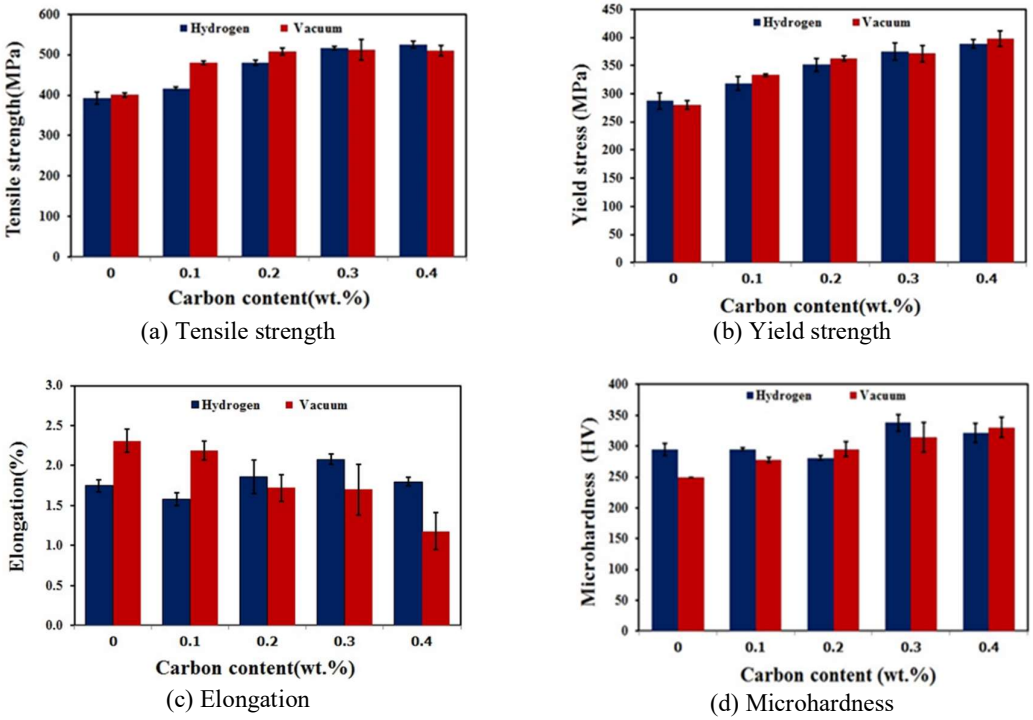

(a) Tensile strength (b) Yield strength

(c) Elongation (d) Microhardness

Figure 5. Mechanical properties of Fe-1.5wt.% Mo + 0.5wt.% h-BN sintered under vacuum and hydrogen atmosphere with variation in C addition.

5. Acknowledgements

Thanks to department of Industrial Physics and Medical Instrumentation (IMI) of Faculty of Applied Science, Lasers and Optics Research Center (LANDOS) of King Mongkut's University of Technology North Bangkok, and grateful for financial supported from National Metal and Materials Technology Center (MTEC), Thailand.

References

[1] P. K. Liao and K. E. Spear, "Alloy phase diagrams," in ASM Handbook, vol. 3, ASM International, Ohio, 1992, pp. 2.8-9.8.

[2] B. Loy and R. J. Dower, "The effect of boron on some properties of sintered iron- carbon alloys," in Proceedings P/M-82, European International Powder Metallurgy Conference, Italy, 1982, pp. 377-391.

[3] T. B. Sercombe, "Sintering of free formed maraging steel with boron additions," *Materials Science and Engineering A*, vol. 363, pp. 242-252, 2003.

[4] M. Sarasola, T. G. Acebo, and F. Castro, "Liquid generation during sintering of Fe-3.5%Mo powder compacts with elemental boron additions," *Acta Materialia*, vol. 52, pp. 4615-4622, 2004.

[5] H. Ö. Gulsoy, "Influence of nickel boride additions on sintering behaviors of injection moulded 17-4 PH stainless steel powder," *Scripta Materialia*, vol. 52, pp.187- 192, 2005.

[6] M. W. Wu, "The influences of carbon and molybdenum on the progress of liquid phase sintering and the microstructure of boron-containing powder metallurgy steel," *Metallurgical and Materials Transactions A*, vol. 46, pp.467-475, 2015.

[7] M. W. Wu, W. Z. Cai, Z. J. Lin, and S. H. Chang, "Liquid phase sintering mechanism and densification behavior of boron-alloyed Fe-Ni-Mo-C-B powder metallurgy steel," *Materials and Design*, vol. 133, pp. 536-548, 2017.

[8] J. Liu, A. Cardamone, T. Potter, R. M. German, and F. J. Semel, "Liquid phase sintering of iron-carbon alloys with boron additions," *Powder Metallurgy*, vol. 43, pp.57-60, 2000.

[9] Z. M. Xiu, "Fe-Mo-B-C sintered steels produced by addition of master alloy powders," *Acta Metallurgica Sinica*, vol. 12, pp. 1198-1201, 1999.

[10] P. Ninpetch, A. Luechaisirikul, M. Morakotjinda, T. Yotkaew, R. Krataitong, N. Tosangthum, S. Mahathanabodee, and R. Tongsri, "Effect of boron nitride on microstructure of Fe-Cr-Mo-BN-C steel sintered in vacuum," *Materials Today: Proceedings*, vol. 5, no.3, pp. 9409-9416, 2018.

[11] M. Tsuda, "Deboronization phenomena in Fe-Ni alloys," *Tetsu-to-Hagane*, vol. 82, pp. 153-158, 1996.

[12] J. Karwan-Baczewska and M. Rosso, "Effect of boron on microstructure and mechanical properties of PM sintered and nitrided steels," *Powder Metallurgy*, vol.44, pp. 221-227, 2001.

[13] M. V. Sundaram, K. B. Surreddi, E. H. Eiga, S. Berg, F. Castro, and L. Nyborg, "Enhanced densification of PM steels by liquid phase sintering with boron-containing master alloy," *Metallurgical and Materials Transactions A*, vol. 49, pp. 255-263, 2018.

[14] A. Hadhud, "Design of reducing agent for sintering of high-performance alloyed PM steels based on different carbon grades analysis," Diploma work No. 95/2012, Chalmers University of Technology, Sweden 2012.

[15] H. I. Aaronson, W. T. Reynolds Jr., and G. R. Purdy, "Coupled-solute drag effects on ferrite formation in Fe-C-X systems," *Metallurgical and Materials Transactions A*, vol. 35, pp.1187-1210, 2004.

[16] M. Momeni, H. Danninger, A. Avakemian, and C. Gierl, "Thermoanalytical sintering studies of Fe-C admixed with ferroboron performed in different atmospheres," *Powder Metallurgy*, vol. 55, pp. 54-64, 2012.

[17] J. Kazior, "The influence of boron on the mechanical properties of prealloyed CrM powders," in Deformation and Fracture in Structural PM Materials (DFPM 2002), Slovakia, 2002, pp.125-131.

[18] J. Wang and S. Van Der Zwaag, "Stabilization mechanisms of retained austenite in transformation-induced plasticity steel," *Metallurgical and Materials Transactions A*, vol. 32, pp. 1527-1539, 2001.

[19] E. Jimenez-Melero, N. H. van Dijk, L. Zhao, J. Sietsma, S. E. Offerman, J. P. Wright, and S. van der Zwaag, "Characterization of individual retained austenite grains and their stability in low-alloyed TRIP steels", *Acta Materialia*, vol. 55, pp. 6713-6723, 2007.

[20] R. Pérez, J. A. Benito, and J. M. Prado, "Study of the inelastic response of TRIP steels after plastic deformation", *ISIJ International*, vol. 45, pp. 1925-1933, 2005.

[21] P. J. Jacques, "Transformation-induced plasticity for high strength formable steels," *Current Opinion in Solid State and Materials Science*, vol. 8, pp. 259-265, 2004.

[22] I. B. Timokhina, P. D. Hodgson, and E. V. Pereloma, "Effect of microstructure on the stability of retained austenite in transformation-induced-plasticity steels," *Metallurgical and Materials Transactions A*, vol. 35, pp. 2331-2341, 2004.